Internal transitions in the confined biexciton

2001 J. Phys.: Condens. Matter 13 L539

(http://iopscience.iop.org/0953-8984/13/23/102)

INSTITUTE OF PHYSICS PUBLISHING JOURNAL OF PHYSICS: CONDENSED MATTER

J. Phys.: Condens. Matter **13** (2001) L539–L544 www.iop.org/Journals/cm PII: S0953-8984(01)24012-0

LETTER TO THE EDITOR

Internal transitions in the confined biexciton

Ricardo Pérez[1,2] **and Augusto Gonzalez**[1,2]

[1] Instituto de Cibernetica, Matematica y Fisica, Calle E 309, Vedado, Ciudad Habana, Cuba
[2] Departamento de Fisica, Universidad de Antioquia, AA 1226, Medellin, Colombia

E-mail: rperez@cidet.icmf.inf.cu (R Pérez) and agonzale@cidet.icmf.inf.cu (A Gonzalez)

Received 18 April 2001

Abstract

Optical internal transitions relevant to experiments based on the optical detection of far-infrared resonances are computed for the biexciton in a quantum dot in the strong-confinement regime. Valence sub-band-mixing effects are taken into account in second-order perturbation theory. The probability of transition from the ground state is concentrated in a few states with relatively high excitation energies. Level collisions with oscillator strength transfer are observed as the magnetic field is raised.

The optical detection of far-infrared resonances [1] (ODR) has proven to be an efficient method in the study of a sector of the exciton spectrum not accessible to inter-band transitions. Far-infrared radiation, in resonance with an internal transition, induces changes in the population of the exciton ground state, changing in this way the amplitude of the luminescence peak. Usually, in order to tune a particular transition into resonance, a magnetic field is used instead of varying the frequency of the infrared source. By this means, many of the exciton transitions as well as electron and hole cyclotron resonance transitions have been clearly observed. In addition to this important result, the two main conclusions to be extracted from reference [1] are the following: (a) with reduced dimensions ODR signals are more pronounced; and (b) experimental transition energies are theoretically reproduced only if valence sub-band-mixing effects are included [2].

On increasing the power of the laser that creates the excitons, new lines corresponding to multiexcitonic transitions are observed. In the present work, we focus on the main biexciton line and address the question of what the main transitions to be observed in an ODR experiment are. As argued below, this question has a non-trivial answer because to many of the low-lying biexciton states there correspond very small transition probabilities, and thus they are very unlikely to be experimentally detected.

Following the dictates of conclusion (a) above, we study the biexciton in a quantum dot in the strong-confinement regime. Very distinct biexcitonic and multiexcitonic lines have been observed in this regime by means of confocal microscopy techniques [3].

Our model quantum dot is disc shaped with a height $w = 8.5$ nm. The in-plane confinement is parabolic [4], with $\hbar\omega_0^e = 7.83$ meV for electrons, leading to a characteristic (oscillator) length of around 12 nm. Oscillator lengths are equal for electrons and holes. This means that $m_{xy}^e\omega_0^e = m_{xy}^{hh}\omega_0^{hh}$, where m_{xy} are the in-plane masses. The Kohn–Luttinger (KL)

0953-8984/01/230539+06$30.00

parameters for GaAs from reference [2] are used: $\gamma_1 = 6.790$, $\gamma_2 = 1.924$, $\gamma_3 = 2.681$, $\kappa = 1.2$ and $q = 0.04$. The relative dielectric constant is $\epsilon = 12.5$.

Hole levels in the dot are computed from the KL Hamiltonian [2,5]. Instead of a numerical diagonalization, we use second-order perturbation theory to account for the non-diagonal terms in the KL Hamiltonian. This kind of approximation has proven to capture many of the actual properties of the hole levels [6]. Keeping the more relevant contributions for thin disc-shaped dots under low magnetic fields, we get for the heavy-hole energies

$$E^{hh}_{n\ell k j_z} = E^0_{n,\ell,k,\pm 3/2} + \left(\frac{8\hbar\gamma_3}{\sqrt{3}m_0\ell_0 w}\right)^2 \Delta E^{\pm} \tag{1}$$

where the unperturbed energies are given by

$$E^0_{n,\ell,k,\pm 3/2} = \frac{\hbar^2\pi^2}{2m^{hh}_z w^2}k^2 + \hbar\Omega^{hh}(2n + |\ell| + 1) - \frac{\hbar\omega^{hh}_c}{2}\ell \pm \mu_B B g^{hh}. \tag{2}$$

n and ℓ are radial and angular momentum projection quantum numbers of the evolving in-plane wave function. k labels the functions along the symmetry axis (z-direction). They are taken as infinite-well functions (assuming, for example, a dot formed from a AlGaAs–GaAs symmetric well with high enough Al concentration). j_z is the total (band) angular momentum projection along z. The effective frequency Ω^{hh} is given by

$$\Omega^{hh} = \sqrt{(\omega^{hh}_c/2)^2 + (\omega^{hh}_0)^2}$$

where ω_c is the cyclotron frequency. m_0 is the electron mass in vacuum, $g^{hh} = 3\kappa + 27q/4 = 3.87$ and

$$\ell_0 = \sqrt{\hbar/(m^e_{xy}\Omega^e)}.$$

Expressions similar to equation (2), in which masses and frequencies are correspondingly replaced and $g^{lh} = \kappa + q/4 = 1.21$, are written for the light hole. The energy corrections, $\Delta E^{\pm}$, where the + refers to $j_z = 3/2$, take the following form:

$$\begin{aligned}
\Delta E^-_{\ell\geqslant 0} &= \frac{n(1+\bar\omega\ell_0^2)^2}{E^0_{n,\ell,1,-3/2} - E^0_{n-1,\ell+1,2,-1/2}} + \frac{(n+\ell+1)(1-\bar\omega\ell_0^2)^2}{E^0_{n,\ell,1,-3/2} - E^0_{n,\ell+1,2,-1/2}} \\
\Delta E^-_{\ell<0} &= \frac{(n+|\ell|)(1+\bar\omega\ell_0^2)^2}{E^0_{n,\ell,1,-3/2} - E^0_{n,\ell+1,2,-1/2}} + \frac{(n+1)(1-\bar\omega\ell_0^2)^2}{E^0_{n,\ell,1,-3/2} - E^0_{n+1,\ell+1,2,-1/2}} \\
\Delta E^+_{\ell>0} &= \frac{(n+1)(1+\bar\omega\ell_0^2)^2}{E^0_{n,\ell,1,3/2} - E^0_{n+1,\ell-1,2,1/2}} + \frac{(n+\ell)(1-\bar\omega\ell_0^2)^2}{E^0_{n,\ell,1,3/2} - E^0_{n,\ell-1,2,1/2}} \\
\Delta E^+_{\ell\leqslant 0} &= \frac{(n+|\ell|+1)(1+\bar\omega\ell_0^2)^2}{E^0_{n,\ell,1,3/2} - E^0_{n,\ell-1,2,1/2}} + \frac{n(1-\bar\omega\ell_0^2)^2}{E^0_{n,\ell,1,3/2} - E^0_{n-1,\ell-1,2,1/2}}
\end{aligned} \tag{3}$$

where $\bar\omega = eB/(2\hbar)$.

The first $j_z = \pm 3/2$ hole energies obtained from an exact diagonalization of the KL Hamiltonian are shown in figure 1 as functions of B. For comparison, the unperturbed values (2) and our approximate energies (1) are also shown, indicating that band-mixing effects may lead to corrections to the single-particle energies of around 1 meV at $B = 5$ T.

Heavy-hole energies from (1) are included in the biexciton Hamiltonian. For the wave function, however, we use the unperturbed functions, neglecting hole mixing[1]. For example,

[1] For the lowest heavy-hole states, the wave function almost coincides with the unperturbed function, and orbital angular momentum can be taken as a good quantum number. Wave-function mixing becomes important at higher excitation energies, where other effects like anharmonicity of the lateral potential and finiteness of the barrier along z may give corrections of the same order to the biexciton energy.

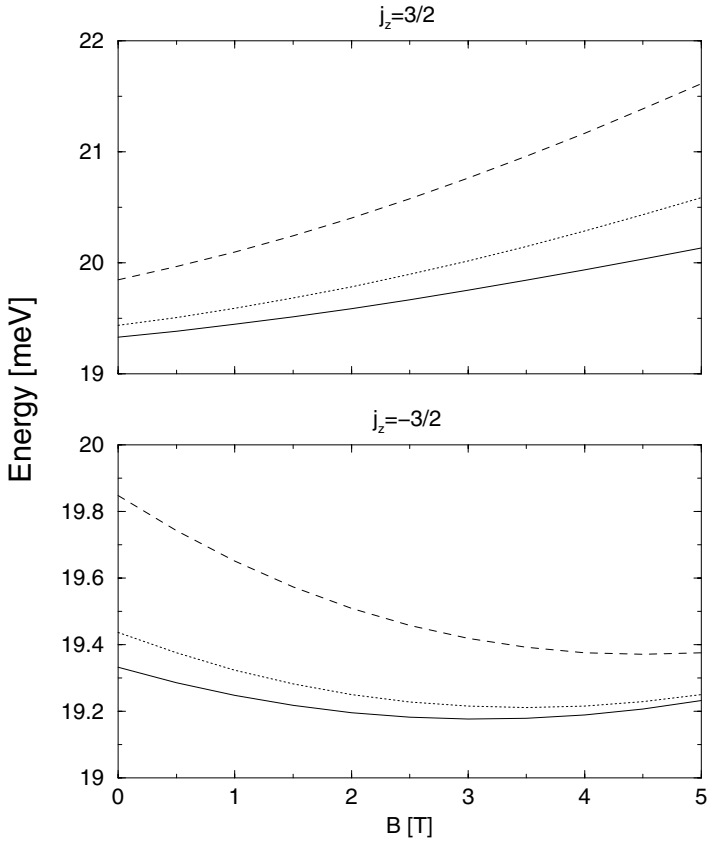

Figure 1. The lowest $j_z = \pm 3/2$ states. Dashed line: equation (2); dotted line: equation (1); and solid line: exact diagonalization of the KL Hamiltonian.

for the state with total electron spin $S_z^e = 1$ and total (band) hole angular momentum $J_z = 3$, which is created by σ^--polarized light, we write the biexciton spatial wave function in the form

$$\Psi_{1,3} = \frac{1}{2}\sum C_{n_1l_1,n_2l_2;n_3l_3,n_4l_4}\{\phi_{n_1l_1}(1)\phi_{n_2l_2}(2) - \phi_{n_1l_1}(2)\phi_{n_2l_2}(1)\} \times \{\phi^{3/2}_{n_3l_3}(3)\phi^{3/2}_{n_4l_4}(4) - \phi^{3/2}_{n_3l_3}(4)\phi^{3/2}_{n_4l_4}(3)\} \tag{4}$$

where indices 1 and 2 refer to electrons, 3 and 4 to holes, and the sum runs over states preserving the total angular momentum projection, $M = l_1 + l_2 + l_3 + l_4$. Up to 16 harmonic oscillator shells, i.e. 136 single-particle states ϕ for electrons and 136 for holes, are included in (4). The resulting large matrices for the biexciton Hamiltonian are diagonalized by means of a Lanczos algorithm.

The results for the first ten transitions from the lowest $S_z^e = 1$, $J_z = 3$ state (an $M = 0$ state), induced by $\sigma^\pm$-polarized far-infrared radiation ($\Delta M = \pm 1$), are presented in figure 2. Levels with more than 10% transition probability are represented by solid lines, and the probability is indicated. Levels with probability less than 10% are represented by dashed lines. We define the normalized probabilities from the expansion coefficient of Ψ_{final} in $D^\pm\Psi_{\text{initial}}$:

$$\text{prob}^\pm = \frac{|\langle\Psi_{\text{final}}|D^\pm|\Psi_{\text{initial}}\rangle|^2}{\langle\Psi_{\text{initial}}|D^-D^+|\Psi_{\text{initial}}\rangle} \tag{5}$$

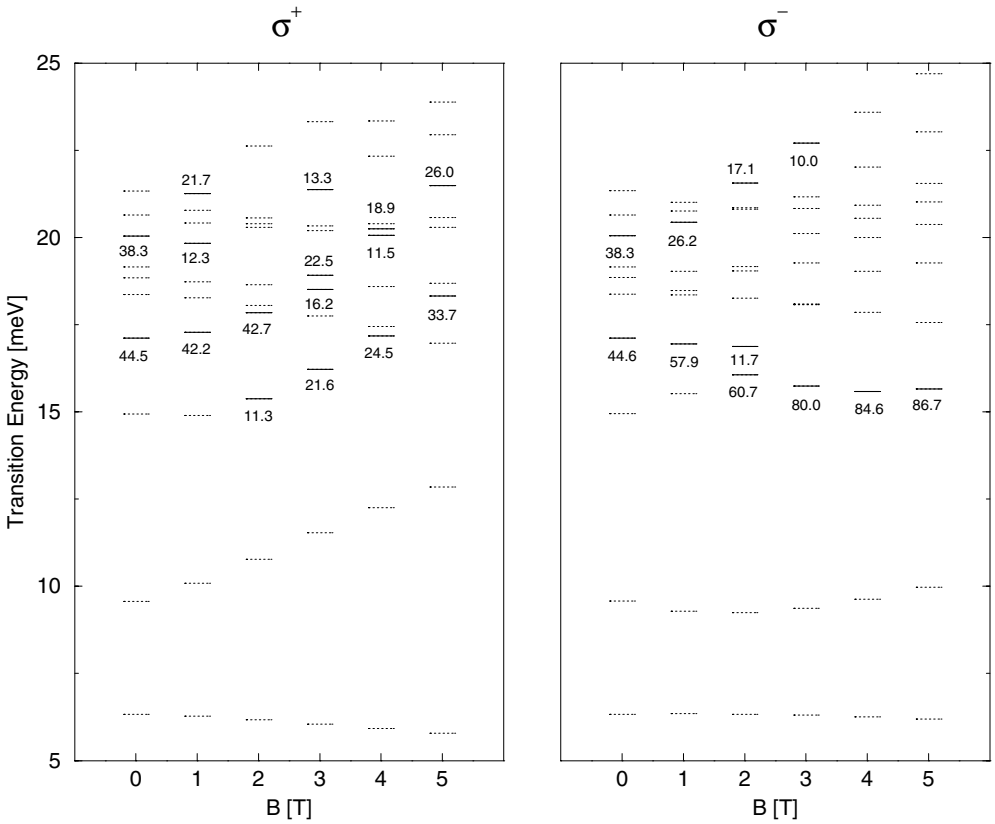

Figure 2. Internal transitions in the $S_z^e = 1$, $J_z = 3$ biexciton. See the explanations in the main text.

where

$$D^{\pm} = r_1 e^{\pm i\theta_1} + r_2 e^{\pm i\theta_2} - r_3 e^{\pm i\theta_3} - r_4 e^{\pm i\theta_4}$$

is the dipole operator for internal $\sigma^{\pm}$-transitions. r, θ are polar coordinates in the plane.

The lowest transitions, with excitation energies below 10 meV, are interpreted as 'single-particle' excitations. Because of their low probabilities, they are unlikely to be detected in an ODR experiment.

Collective motions, in which the electron cloud oscillates in counterphase with respect to the hole cloud, account for most of the transition probability. Their excitation energies take values between 15 and 20 meV (the solid lines). In the biexciton, they are small-scale versions of the giant-dipole resonances expected for larger multiexcitonic systems [7]. Because of the difference between electron and hole masses and the magnetic field, the dipole resonance splits into a few states. The two transitions indicated at $B = 0$, for example, account for 83% of the probability. At $B = 5$ T, there are two states accounting for 60% of the σ^+-transition probability and a single state accounting for 87% of the σ^--probability.

Basically, these dipole excitations are the ones to be registered by means of ODR. Following only the solid lines, one may notice in σ^-:

(i) a 'state' with constant excitation energy around 16 meV whose ODR signal becomes very strong as B is increased; and
(ii) a state starting at around 20 meV whose excitation energy rises abruptly for $B > 1$ T;

whereas for σ^+ we may distinguish:

(iii) a state clearly seen for $B \geqslant 2$ T starting at $\Delta E \approx 15$ meV and whose ODR signal increases;

(iv) a state starting at $\Delta E \approx 17$ meV with a very strong ODR signal at low B which decreases at higher B; and, finally,

(v) a state starting at $\Delta E \approx 20$ meV whose ODR signal diffuses as B is raised.

The energy of all of the $M = 1$ states increases with B.

A careful examination of the transitions shown in figure 2 reveals a complex pattern of probability transfer as the magnetic field is raised. For example, let us look at the three 'colliding' levels at excitation energies around 18 meV for σ^+-polarization and $B = 2$ T. The transition probabilities are 42.7, 0.3 and 1.0% from bottom to top. After the collision, i.e. at $B = 3$ T, the probabilities become 0.0, 16.2 and 22.5% respectively. This means that ODR signals may experience significant changes even with relatively small variations of B.

Similar results are presented in figure 3 for the singlet (electron), $J_z = 0$ biexciton. The lowest state in this sector is also an $M = 0$ state. Low-lying $M = \pm 1$ dark levels, a ~15 meV gap to the dipole resonances and a complex pattern of probability transfer with increasing magnetic field are also evident in this figure.

In conclusion, we have computed the lowest-lying energy levels and transition probabilities relevant for the ODR study of the biexciton in a quantum dot. The states that will induce

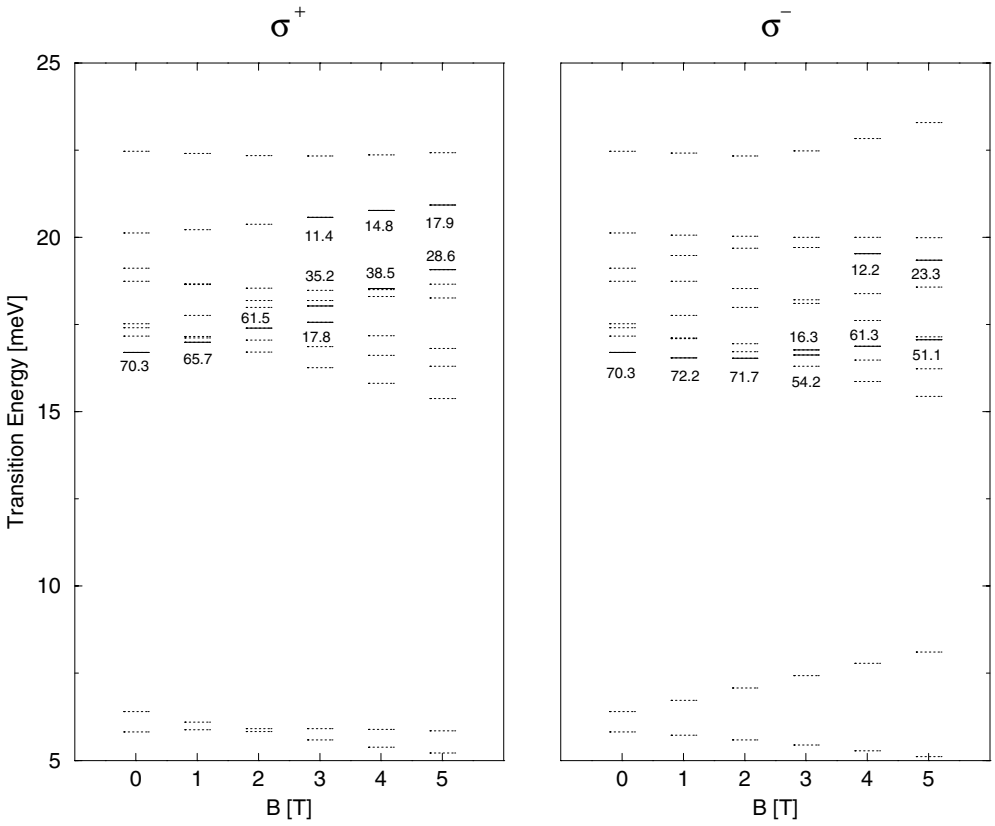

Figure 3. As figure 2, but for the singlet (electron), $J_z = 0$ biexciton.

the most pronounced ODR signals are collective dipole excitations, with excitation energies higher than $\hbar(\omega_0^e + \omega_0^{hh})$. A complex dependence of the transition probabilities on B, leading to significant variations of the position and depth of ODR signals, is predicted.

The authors acknowledge support by the Committee for Research (CODI) of the University of Antioquia and by the Caribbean Network for Theoretical Physics. Useful discussions with B Rodriguez are gratefully acknowledged.

References

[1] Cerne J *et al* 1996 *Phys. Rev. Lett.* **77** 1131
Salib M S *et al* 1996 *Phys. Rev. Lett.* **77** 1135
Nickel H A *et al* 2000 *Phys. Rev.* B **62** 2773
[2] Bauer G E W and Ando T 1988 *Phys. Rev.* B **38** 6015
[3] Dekel E *et al* 1998 *Phys. Rev. Lett.* **80** 4991
Dekel E *et al* 2001 *Solid State Commun.* **117** 395
Biexcitonic effects in the opposite, weak-confinement, regime were studied by
Kamada H *et al* 1998 *Phys. Rev.* B **58** 16 243
[4] This is a common model for self-assembled or strained dots; see for example
Jacak L, Hawrylak P and Wojs A 1998 *Quantum Dots* (Berlin: Springer)
Effective dots in quantum wells arising from width fluctuations have also been modelled with a parabolic confinement; see for example
Riva C *et al* 1998 *Phys. Status Solidi* b **210** 689
[5] Luttinger J M and Kohn W 1955 *Phys. Rev.* **97** 869
Luttinger J M 1956 *Phys. Rev.* **102** 1030
[6] Brasken M, Lindberg M and Tulkki J 1997 *Phys. Rev.* B **55** 9275
[7] Delgado A, Lavin L, Capote R and Gonzalez A 2000 *Physica* E **8** 342